Available online at www.sciencedirect.com
SCIENCE DIRECT
Thermochimica Acta 437 (2005) 48–58
thermochimica acta
www.elsevier.com/locate/tca

Study of the dichromate-catalysed hydrogen peroxide decomposition: Comparison of different batch mode reactors for the kinetics determination

Nader Frikha [a,*], Eric Schaer [b], Jean-Léon Houzelot [a]

[a] *Laboratoire des Sciences du Génie Chimique, CNRS, Ecole Nationale Supérieure des Industries Chimiques, INPL, 1, rue Grandville, BP 451, 54001 NANCY Cedex, France*
[b] *Centre de Génie Chimique des Milieux Rhéologiquement Complexes, CNRS, Ecole Nationale Supérieure des Industries Chimiques, INPL, 1, rue Grandville, BP 451, 54001 NANCY Cedex, France*

Received 8 March 2005; received in revised form 31 May 2005; accepted 6 June 2005
Available online 15 July 2005

Abstract

This paper deals with an experimental batch mode study of a chemical homogeneous reaction: the dichromate-catalysed hydrogen peroxide decomposition. The thermodynamic properties and the kinetic parameters of the reaction are simultaneously determined using a calorimetric approach. Various batch-operating modes (adiabatic, isoperibolic, or differential thermal analysis) are compared and it is shown that the determined parameters do not depend on the operating mode. A complete kinetic law is proposed. The reaction rate constant is assumed to follow the Arrhenius rate law. The Arrhenius parameters are determined as frequency factor $k_0 = 1.39 \times 10^9\ s^{-1}$ and activation energy $E = 54.9\ kJ\ mol^{-1}$. The measured enthalpy of reaction is $\Delta_r H = -94\ kJ\ mol^{-1}$. The reaction order is between 0 and 2 in hydrogen peroxide according to operating conditions and depends linearly on the initial dichromate concentration. The reaction can be managed by two parameters: on one hand the released reaction heat directly depends on the hydrogen peroxide concentration, and on the other hand, the kinetic rate can be increased in increasing the dichromate concentration.

Keywords: Hydrogen peroxide decomposition; Batch mode kinetics study; Adiabatic reactor; Isoperibolic reactor; Differential thermal analysis reactors

1. Introduction

The determination of reaction kinetics is of major importance, as for industrial reactors optimization as for environmental reasons or energy limitations. Kinetics determination is traditionally carried out in batch mode, and the reactor must then be equipped for the concentrations variations measurements [1]. When reaction is exo- or endothermic, the temperature measurements alone makes it possible to follow the conversion or reaction extend against time.

Reaction calorimetry, i.e. measurement in energy release or uptake during a reaction, is a scientific tool designed for measurement of thermodynamic parameters: specific heat, latent heat, calorific powers, enthalpy of reaction or transformation. Calorimetry is perhaps one of the oldest scientific known technologies, with published examples dating back to the 18th century [2]. Recently, reaction calorimetry has expanded to find a variety of uses in process development, process safety and basic research [3–5].

While calorimetry is very often used for the determination of thermodynamics parameters alone, the resolution of the coupled heat and mass balances also allows the determination of kinetics parameters.

The objective of this study consists in using a calorimetric approach for the simultaneous determination of thermody-

* Corresponding author. Tel.: +33 3 83 17 50 88; fax: +33 3 83 17 50 86.
E-mail address: Nader.Frikha@ensic.inpl-nancy.fr (N. Frikha).

0040-6031/$ – see front matter © 2005 Elsevier B.V. All rights reserved.
doi:10.1016/j.tca.2005.06.017

Nomenclature

A	heat transfer area (m^2)
C_p	specific heat capacity ($J\,kg^{-1}\,K^{-1}$)
d_{am}	mean absolute difference (K)
E	activation energy ($J\,mol^{-1}$)
k	rate constant (s^{-1})
k_0	frequency factor (s^{-1})
K	equilibrium constant ($L^2\,mol^{-2}$)
m	mass (kg)
n	number of experimental and/or calculated points
n_j	moles of component j (mol)
P	power (W)
r	reaction rate ($mol\,L^{-1}\,s^{-1}$)
T	temperature (K)
U	overall heat transfer coefficient ($W\,m^{-2}\,K^{-1}$)
V	volume (L)
X	conversion (–)

Greek letters

α	reaction order (–)
ΔG°	$(=\Delta H^\circ - T\Delta S^\circ)$ molar free energy of formation of $Cr_2O_9^{2-}$
$\Delta_r H$	enthalpy of reaction ($J\,mol^{-1}$)
ΔT_{ad}	adiabatic temperature rise (K)
ν_j	stoichiometric coefficient of component j (–)
ρ	density ($kg\,m^{-3}$)
σ	relative standard deviation (–)
τ_c	thermal constant (s)
φ	thermal inertia (–)

Superscripts

max	maximal value

Subscripts

ad	adiabatic
amb	ambient
calc	calculated
d	differential
exp	experimental
reactants	reactants
reactor	reactor
th	theoretical
w	wall
0	initial

namic and kinetic parameters. The method is applied to the dichromate-catalysed hydrogen peroxide decomposition, and several experimental devices are compared: batch adiabatic reactor, batch non-adiabatic reactor (or isoperibolic reactor) and batch reactor functioning according to the differential thermal analysis principle.

2. Dichromate-catalysed hydrogen peroxide decomposition

This reaction was selected according to its simplicity of implementation. It is also based on the use of non-toxic reactants and products, therefore without serious consequences in the event of accidental thermal runaway. Lastly, it was not the subject of any complete kinetic study, which testifies for the interest of this work.

This reaction was the object of some previous studies [6–8], and involves the following stoichiometric mechanism:

$$2H_2O_2 + Cr_2O_7^{2-} \overset{K}{\longleftrightarrow} Cr_2O_9^{2-} + 2H_2O$$

$$Cr_2O_7^{2-} \xrightarrow{k'} Cr_2O_7^{2-} + O_2 \quad (1)$$

Kobozev et al. [7] reported that there are doubts on the true form of the intermediate ion ($Cr_2O_9^{2-}$and/or $HCrO_6^-$), but Brungs et al. [8] asserts that this does not have any influence on the determination of the kinetics expressions.

Indeed, assuming the first stage is fast and balanced, and the second slower one establishes the kinetic determining step [9], of order α:

$$K = \frac{[Cr_2O_9^{2-}]}{[Cr_2O_7^{2-}]\,[H_2O_2]^2}, \qquad r_{Cr} = k'[Cr_2O_9^{2-}]^\alpha \quad (2)$$

the dichromate molar conservation:

$$\left\lfloor Cr_2O_7^{2-} \right\rfloor_0 = \left\lfloor Cr_2O_7^{2-} \right\rfloor + \left\lfloor Cr_2O_9^{2-} \right\rfloor \quad (3)$$

leads to:

$$[Cr_2O_9^{2-}] = \frac{K[H_2O_2]^2[Cr_2O_7^{2-}]_0}{1 + K[H_2O_2]^2} \quad (4)$$

Finally, the consumption rate of dichromate is half of that of peroxide. The kinetic expression of the dichromate-catalysed hydrogen peroxide decomposition can then be expressed as:

$$r_{H_2O_2} = 2r_{Cr} = 2k'[Cr_2O_9^{2-}]^\alpha = k[Cr_2O_9^{2-}]^\alpha = k\left(\frac{K[H_2O_2]^2[Cr_2O_7^{2-}]_0}{1 + K[H_2O_2]^2}\right)^\alpha \quad (5)$$

Thus, the kinetics does not depend on the form of intermediate ions in the solution, but on the sum of their concentrations, corresponding to the total initial dichromate concentration.

The reaction order α is traditionally said to be 1 in the literature [6–8]. This will be confirmed in the experimental part of this work. In this case, the kinetic expression takes the general form:

$$r = k\frac{K[H_2O_2]^2[Cr_2O_7^{2-}]_0}{1 + K[H_2O_2]^2} \quad (6)$$

According to experimental conditions, the kinetic expression can take a simplified form. Indeed with strong hydrogen

peroxide concentrations, it becomes of pseudo zeroth order in this reactant:

$$r = k\left[\mathrm{Cr_2O_7^{2-}}\right]_0 \tag{7}$$

3. Experimental determination of thermodynamic and kinetic parameters

This part deals with the general methodology of thermodynamic and kinetic parameters determination. The thermal characterization of the reactor is approached, and heat and mass balance are then detailed.

3.1. Thermal characterization

Whatever the type of reactor used for the thermodynamic and kinetic determination, this one may not be perfectly adiabatic. In this case, the thermal characteristics of the reactor are first determined using a traditional calorimetric measurement. The procedure consists in heating the reactor contents by a thermal source (generally an electric resistance) and to follow the temperature evolution against time.

The determined thermal characteristics are here:

- the overall heat transfer coefficient U, which accounts for the eventual heat losses,
- the thermal inertia φ such as $\varphi = 1 + \frac{m_{\text{reactor}} C_{\text{p}_{\text{reactor}}}}{m_{\text{reactants}} C_{\text{p}_{\text{reactants}}}}$, which accounts for the reactor's heat capacity. φ is the ratio of the total heat flow, necessary for the heating of the reactants and the reactor, to the reactants heat flow.

Defining T_w as the extern or jacket temperature, P as the power of a thermal source and A as the heat transfer area, that is to say the measured wet area in contact with the reactor walls, the resolution of heat balance in batch mode [10] allows the determination of the thermal characteristics:

$$UA(T_\text{w} - T) = m_{\text{reactants}} C_{\text{p}_{\text{reactants}}} \varphi \frac{\mathrm{d}T}{\mathrm{d}t} - P \tag{8}$$

Resolution of Eq. (8) was numerically performed using Matlab. The least square difference between calculated and measured temperatures was minimized using the subroutine 'fminsearch' that finds the minimum of a function of several variables and making it possible to identify the two parameters U and φ.

3.2. Heat and mass balances

The hydrogen peroxide decomposition releases some oxygen as reaction proceeds and the reactional volume could then vary between the beginning and the end of an experiment. For this reason, it has been chosen to work with moderate concentrations and temperatures, to minimize the volume variation and the evaporation heat losses.

Indeed, the peroxide concentration is then between 0.45 and 2.7 M, and the dichromate concentration remains lower than 0.01 M. Under these conditions the variation of volume lies between 0.25 and 1.5% and the variation of the total heat capacity is between 0.11 and 0.64%. Furthermore, the heat flow corresponding to the evaporation of the components of the reactional medium can be theoretically estimated. It remains very small, and does not exceed 2% of the other exchanged heat flows. Thus, the volume variation is not significant and the evaporation heat losses remain negligible.

In this case, for a simple stoichiometry reaction, implemented in batch mode, the heat and mass balance lead to:

$$\frac{\mathrm{d}n_j}{\mathrm{d}t} = \nu_j r V \tag{9}$$

$$UA(T_\text{w} - T) = m_{\text{reactants}} C_{\text{p}_{\text{reactants}}} \varphi \frac{\mathrm{d}T}{\mathrm{d}t} + rV\,\Delta_\text{r}H \tag{10}$$

The batch adiabatic mode, when it is possible to carry the reaction out without any risk of thermal runaway, is undoubtedly the simplest to use because it leads to a simple relation between temperature and conversion.

Some other batch modes, which ensure the dissipation of the heat of reaction, are often preferred for security reasons (isoperibolic reactor...). Even if the relation between temperature and conversion is then less direct, it is possible to analyze the obtained results, to express conversion and temperature against time, and finally to specify the reaction kinetics, by resolution of heat and mass balance equations.

Thereafter, the reaction will be initially studied in adiabatic mode. The results will be confronted with those obtained for different non-adiabatic batch modes, such as isoperibolic mode or differential thermal analysis mode.

4. Batch adiabatic reactor

Adiabatic operating mode is characterized by a low thermal inertia ($\varphi \approx 1$) and low heat loss conditions [4]. Study in this mode is a stage of reaction assessment, and is normally undertaken to quantify the energy release or uptake during a reaction and deduce reactional kinetics and thermodynamics parameters.

4.1. Protocol

The batch adiabatic reactor was here a Dewar vessel of 1 L capacity. It was not exactly adiabatic, since it exchanges heat with outside through its higher part. The heat transfer properties were evaluated from calibrations performed with the initial and final reaction masses. Since the values were approximately the same, UA and φ were considered constant during the reaction. It allowed estimating the overall heat transfer coefficient UA to 0.27 W K^{-1}, and the thermal inertia φ to 1.08.

The reactants were purchased from Prolabo and were used as received. The purity of the potassium dichromate

is higher than 99.9 % and the concentration of hydrogen peroxide is 9.82 M (110 V). Two separated potassium dichromate and hydrogen peroxide solutions were then prepared. Volumes of these solutions were selected to keep a total final volume of 0.5 L and to obtain defined concentrations after mixture. The hydrogen peroxide solution was first loaded, and agitated at 700 rpm. Once the desired initial temperature was reached, the dichromate solution was rapidly added using a micropipette. The dichromate concentration is much lower than that of peroxide, so the dichromate volume is small compared to that of peroxide (less than 3 %) and its dispersion in the solution can be considered as instantaneous. Agitation was continuously ensured by a Rushton turbine, whose stirring speed is maintained at 700 rpm.

The temperature variation versus time, with an acquisition rate of 10 points per second, was finally recorded.

4.2. Exploitation of temperature curves

It has been choosen to define conversion X according to hydrogen peroxide, since dichromate is regenerated as reaction proceeds, as shown by the reactional mechanism (1). ΔT_{ad} is the adiabatic temperature rise:

$$[H_2O_2] = [H_2O_2]_0(1 - X),$$

$$\Delta T_{ad} = \frac{[H_2O_2]_0(-\Delta_r H)}{\rho_{reactants} C_{p_{reactants}}} \tag{11}$$

The mass and heat balance here become:

$$r = -\frac{d[H_2O_2]}{dt} = [H_2O_2]_0 \frac{dX}{dt} \tag{12}$$

$$UA(T_{amb} - T) = m_{reactants} C_{p_{reactants}} \varphi \frac{dT}{dt} + rV\,\Delta_r H \tag{13}$$

where T_{amb} is the ambient temperature.

Defining τ_c as a characteristic thermal constant:

$$\tau_c = \frac{m_{reactants} C_{p_{reactants}}}{UA} \tag{14}$$

The heat balance is easily rearranged into:

$$\frac{dT}{dt} = \frac{(T_{amb} - T)}{\tau_c \varphi} + \frac{\Delta T_{ad}}{\varphi} \frac{dX}{dt} \tag{15}$$

which can finally be integrated as:

$$\frac{\Delta T_{ad}}{\varphi} X = (T - T_0) + \int_0^t \frac{T - T_{amb}}{\tau_c \varphi} \tag{16}$$

Using this last expression, an "adiabatic temperature" T_{ad}, which corresponds to the temperature variation that could be obtained in adiabatic mode without any heat loss, can numerically be calculated:

$$T_{ad} = T_0 + \Delta T_{ad} X = T_0 + \varphi(T - T_0) + \int_0^t \frac{T - T_{amb}}{\tau_c} \tag{17}$$

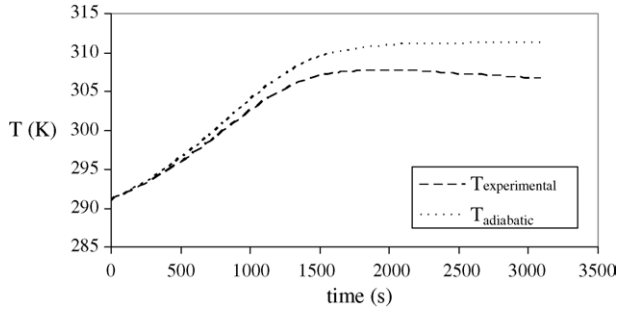

Fig. 1. Temperatures variations in batch adiabatic mode. $T_0 = 291$ K; $[H_2O_2]_0 = 0.9$ M; $[Cr_2O_7]_0 = 0.003$ M.

The variations of measured and adiabatic temperatures in batch adiabatic mode are presented in Fig. 1. The two temperatures are very close, especially at the beginning of the reaction, showing that heat losses remain very small. The adiabatic temperature does not correspond to any real temperature in the Dewar; it simply makes it possible to precise the end of the reaction (when it does not vary any more), to calculate the adiabatic temperature rise, and translates the conversion variations against time.

The numerical value of the adiabatic temperature rise ΔT_{ad} can then be calculated from Fig. 1, and the conversion is also easily deduced:

$$\Delta T_{ad} = T_{ad}^{max} - T_0, \qquad X = \frac{T_{ad} - T_0}{\Delta T_{ad}} \tag{18}$$

4.3. Variation of process parameters

This part describes the influence of several process parameters on the dichromate-catalysed hydrogen peroxide decomposition. The following figures present the calculated adiabatic temperature variations versus time, for different operating conditions.

4.3.1. Initial temperature

Fig. 2 presents the adiabatic temperature variations as a function of time for different initial temperatures, and initial concentrations of 0.003 M for dichromate and of 1.8 M for peroxide.

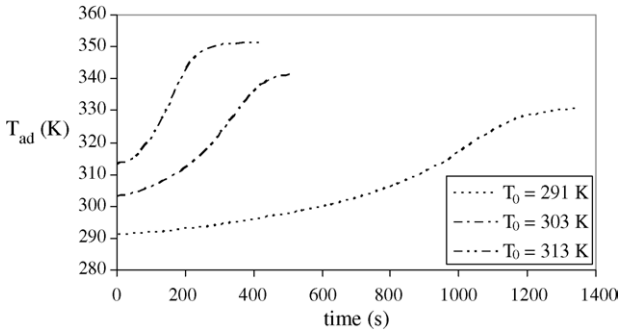

Fig. 2. Adiabatic temperatures variations for different initial temperatures. $[H_2O_2]_0 = 1.8$ M; $[Cr_2O_7]_0 = 0.003$ M.

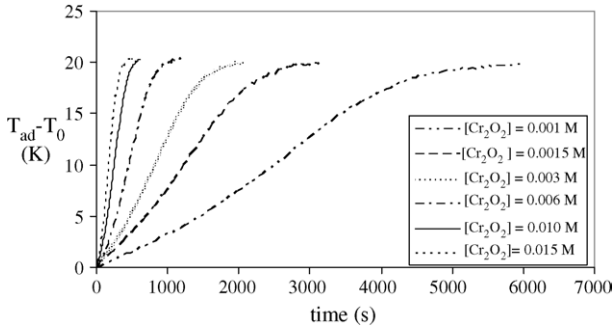

Fig. 3. Influence of dichromate concentration. T_0 = 291 K; $[H_2O_2]_0$ = 0.9 M.

The reaction is accelerated by an increase of the initial temperature, which logically corresponds to the dependence of the rate constant against temperature, according to the Arrhenius law. It can also be remarked that the temperature variation is linear at the beginning of the reaction, and it is thus possible to determine an initial reaction rate:

$$r_0 = [H_2O_2]_0 \left.\frac{dX}{dt}\right|_{t=0} = [H_2O_2]_0 \frac{1}{\Delta T_{ad}} \left.\frac{dT_{ad}}{dt}\right|_{t=0} \quad (19)$$

4.3.2. Dichromate concentration

Fig. 3 presents the influence of the dichromate concentration on the temperature, for an initial peroxide concentration of 0.9 M.

It can be seen that the reaction rate increases with the dichromate concentration. It is also remarked that the maximal variation in temperature ΔT_{ad} remains the same, which translates that dichromate only modifies the reaction rate: the adiabatic temperature rise only depends on the peroxide concentration. Lastly, it can be noticed that the variations of temperature versus time are rather linear at the beginning of the reaction, and that they change at the end of the experiment i.e. for smaller hydrogen peroxide concentrations.

Fig. 4 presents the variations of initial slopes dT_{ad}/dt (which according to relation 19 is directly proportional to the initial consumption rate of peroxide, since $[H_2O_2]_0$ and ΔT_{ad} remain unchanged), as a function of the initial dichromate concentration. The linear variation confirms that the initial rate is proportional to the initial dichromate concentration.

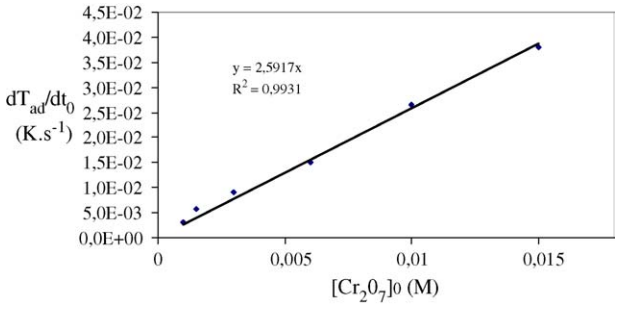

Fig. 4. Initial variation rates of adiabatic temperature vs. dichromate concentration. T_0 = 291 K; $[H_2O_2]_0$ = 0.9 M.

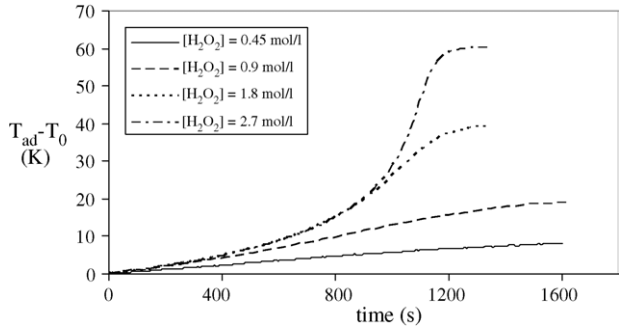

Fig. 5. Influence of initial hydrogen peroxide concentration. T_0 = 291 K; $[Cr_2O_7]_0$ = 0.003 M.

4.3.3. Hydrogen peroxide concentration

The dichromate concentration was here kept constant, while varying the initial hydrogen peroxide concentration. Fig. 5 shows that the reaction is zeroth order in peroxide for the large hydrogen peroxide concentrations: indeed it can be noted that initial rates all are identical, thus independent of the initial hydrogen peroxide concentration.

Initial temperature variation rates (proportional to the initial reaction rate, according to relation 19) are presented in Table 1. The almost similar values, for large initial peroxide concentrations, show that the initial kinetics does not depend on peroxide concentration. Indeed, for large peroxide concentration, the kinetics becomes of pseudo zeroth order in peroxide (see relations 6 and 7) and reaction rate just depends on dichromate concentration. For lower peroxide concentrations, the $K[H_2O_2]^2$ term becomes of the same order of magnitude as 1 (see again relations 6 and 7) and temperature variation rates (and kinetics) thus depend on peroxide concentration.

On an other hand, it can be confirmed that the adiabatic temperature rise depends on the peroxide concentration.

4.3.4. Conclusion

The variation of experimental conditions showed that the kinetics is activated by temperature, does not depend initially on (large) peroxide concentration and is proportional to the initial dichromate concentration. The next part concerns the determination of thermodynamics and kinetics parameters.

4.4. Determination of enthalpy and kinetics expression

4.4.1. Enthalpy of reaction

The enthalpy of reaction $\Delta_r H$ is deduced from the experimental values of the adiabatic temperature rise ΔT_{ad}. Com-

Table 1
Initial temperature variations rates against time

Initial peroxide concentration (M)	$\left.\frac{dT_{ad}}{dt}\right\|_{t=0}$ (K s^{-1})
0.45	0.0057
0.9	0.0090
1.8	0.0103
2.7	0.0105

Table 2
Molar enthalpy of reaction for different dichromate concentrations

$[Cr_2O_7]_0$ (M)	$-\Delta_r H$ (kJ/mol)
0.001	93.8
0.0015	92.8
0.003	95.4
0.006	94.4
0.01	96.3
0.015	94.6

pared values of enthalpy are presented in Table 2. The mean enthalpy value, for varying operating conditions and reproducibility experiments is:

$$\Delta_r H = -94.6\,\mathrm{kJ\,mol^{-1}}$$

The enthalpy value is related to the peroxide mole number, with 2.3% of uncertainty.

4.4.2. Kinetics expression

The kinetic model depends on four parameters:

- two for the rate constant, described according to the Arrhenius law:

$$k = k_0 \exp\left(-\frac{E}{RT}\right) \tag{20}$$

where E is the activation energy of the reaction,

- and two for the equilibrium constant:

$$K = \exp\left(-\frac{\Delta G^\circ}{RT}\right) \tag{21}$$

where ΔG° is the free molar energy of formation of $Cr_2O_9^{2-}$. The Ellingham approximation, which consists in linearizing ΔG° is here supposed. Thus, for the experimental temperature variation range (293–323 K), the free energy of formation of $Cr_2O_9^{2-}$ can be described as:

$$\Delta G^\circ(T) = \Delta H^\circ(T_0) - T\Delta S^\circ(T_0) \tag{22}$$

where $\Delta H^\circ(T_0)$ and $\Delta S^\circ(T_0)$ are respectively the enthalpy and entropy of formation of $Cr_2O_9^{2-}$ at $T_0 = 298$ K.

The simultaneous identification of four parameters is very delicate and cannot give precise results without initial estimates of the parameters. For this reason, the equilibrium constant was first estimated according initial experimental rates.

Indeed, the kinetics expression (6) shows that $1/r$ varies linearly against $1/[H_2O_2]^2$:

$$\frac{1}{r} = \frac{1}{kK[Cr_2O_7^{2-}]_0}\frac{1}{[H_2O_2]^2} + \frac{1}{k[Cr_2O_7^{2-}]_0} = a\frac{1}{[H_2O_2]^2} + b \tag{23}$$

So, the equilibrium constant can be estimated from the b/a ratio.

Equilibrium constant K was first estimated from relation 23, applied to initial reaction rates. The initial reaction rates

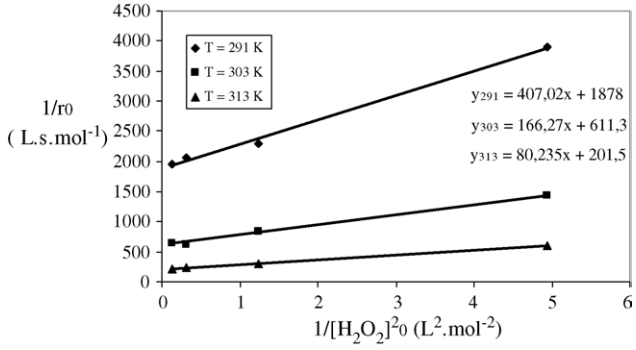

Fig. 6. Reciprocal of initial rates against reciprocal squared initial concentrations of hydrogen peroxide for different temperatures. $[Cr_2O_7]_0 = 0.003$ M.

are easily deduced from adiabatic temperature variations, using relation 19. Fig. 6 presents the variations of reciprocal initial rates versus reciprocal squared initial hydrogen peroxide concentrations. The equilibrium constant is then deduced, for each temperature, from the slope and intercept. The logarithmic variations of K against $-1/T$ are finally presented in Fig. 7. The initial expression of the equilibrium constant K is then:

$$K\,(\mathrm{L^2\,mol^{-2}}) = \exp\left(\frac{2480}{T} - 6.957\right) \tag{24}$$

This method is not very precise, because of the lack of precision on the graphic determination of initial rates and because only three data points were used for the determination of the linear relationship. However, the initial value of the equilibrium constant thus determined just gives an order of magnitude of this parameter, which will be useful for its exact determination.

The kinetic identification was finally carried out by coupled resolution of heat and mass balances for the performed experiments. The differential equations (9) and (10) being non-linear, an exact analytical solution cannot be obtained and numerical techniques are required to deduce kinetics parameters. The set of mass and heat balances (expressed as a function of X and T, Eqs. (25) and (26)) was solved using a Matlab® explicit Runge–Kutta method 'ode45'. The relative least square difference between calculated and exper-

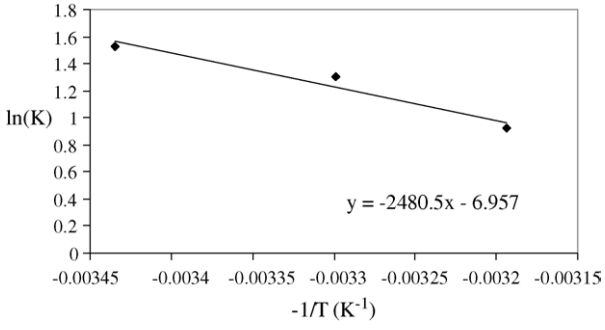

Fig. 7. Temperature dependency of the experimental equilibrium constant. $[Cr_2O_7]_0 = 0.003$ M.

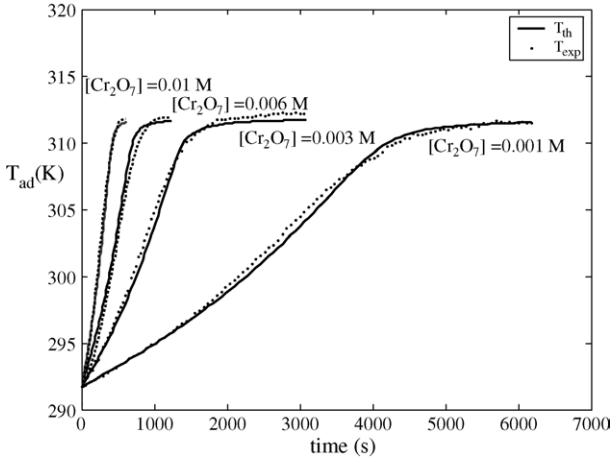

Fig. 8. Experimental and theoretical adiabatic temperatures. $[H_2O_2]_0 = 0.9$ M.

imental temperatures was optimized using the subroutine 'fminsearch' that finds the minimum of a scalar function of several variables (i.e. 2 for k and 2 for K), starting at an initial estimate. This is generally referred to as unconstrained non-linear optimization [11]. The optimization was simultaneously realised on all the performed experiments. Several optimization runs were successively performed, for different starting values. Depending on the initial values of the kinetic and equilibrium parameters, the number of optimizations runs had to vary to give same final optimized relative least square difference and values of k and K. Thus, the optimal solution does not depend on initial values (but the number of runs to perform does), testifying for the quality of the optimized values:

$$\frac{dT}{dt} = \frac{(T_{amb} - T)}{\tau_c \varphi} + \frac{\Delta T_{ad}}{\varphi}\frac{dX}{dt} \tag{25}$$

$$\frac{dX}{dt} = \frac{kK[H_2O_2]_0[Cr_2O_7{}^{2-}]_0(1-X)^2}{1 + K[H_2O_2]_0^2(1-X)^2} \tag{26}$$

Fig. 8 shows that the agreement is very satisfactory and makes it possible to identify the kinetic and equilibrium parameters. The optimized value of K, and particularly its enthalpy of formation, is rather different of the initial value, what shows the interest of a complete optimisation:

$$k\,(s^{-1}) = 2.53 \times 10^9 \exp\left(-\frac{6920}{T}\right),$$

$$K\,(L^2\,mol^{-2}) = \exp\left(\frac{2776}{T} - 5.19\right) \tag{27}$$

The uncertainty between calculated and experimental temperatures can be described using a relative standard deviation as:

$$\sigma = \left(\frac{1}{n}\sum_n \left(\frac{T_{exp} - T_{calc}}{T_{exp}}\right)^2\right)^{1/2} \tag{28}$$

or a mean absolute difference, expressed in Kelvin:

$$d_{am} = \frac{1}{n}\sum_n \left|T_{exp} - T_{calc}\right| \tag{29}$$

where n is the number of experimental and calculated points.

For the set of optimized parameters in batch adiabatic mode, the relative standard deviation is here 1.6×10^{-3} and the mean absolute difference is 0.39 K.

4.5. Conclusion

The dichromate-catalysed decomposition of hydrogen peroxide has been fully characterized in batch adiabatic mode. The reaction kinetics depends linearly on the initial dichromate concentration. Its order in hydrogen peroxide varies between 0 and 2, and reduces to a pseudo zeroth order for large hydrogen peroxide concentrations. The activation energy E is 57.6 kJ mol^{-1} and the heat released (or the adiabatic temperature rise) depends on the initial peroxide concentration. Equilibrium parameters are determined as $\Delta H^\circ(T_0) = -23.1$ kJ mol^{-1} and $\Delta S^\circ(T_0) = -43.1$ J mol^{-1}.The following kinetic model can finally be proposed:

$$r = \frac{1.39 \times 10^9 \exp\left(-\frac{5.76\times10^4}{RT}\right)\exp\left(\frac{2776}{T} - 5.19\right)[H_2O_2]^2[Cr_2O_7{}^{2-}]_0}{1 + \exp\left(\frac{2776}{T} - 5.19\right)[H_2O_2]^2} \tag{30}$$

5. Batch isoperibolic reactor

If the reaction is too exothermic, it is often preferable to carry it out in a batch-jacketed vessel, with constant wall temperature, i.e. in isoperibolic mode where the reaction heat is easily dissipated. In addition, when the determination of kinetics must be made in absence of any calorimeter (for example on a factory site, in the production reactor) this section confirms that the use of isoperibolic mode allows the precise determination of kinetic laws.

5.1. Protocol

The reaction was here carried out in a 0.25 L capacity jacketed vessel, whose jacket temperature T_w is maintained constant using a cooling bath. The reactor used is made of borosilicate and were purchased from Dilvac. The thermal calibration was realized as in the batch adiabatic mode. Resolution of the calibration balance (relation 8) gives here: $UA = 5.97$ W K^{-1} and $\varphi = 1.057$. The reaction was started after addition of a small quantity of dichromate solution. The

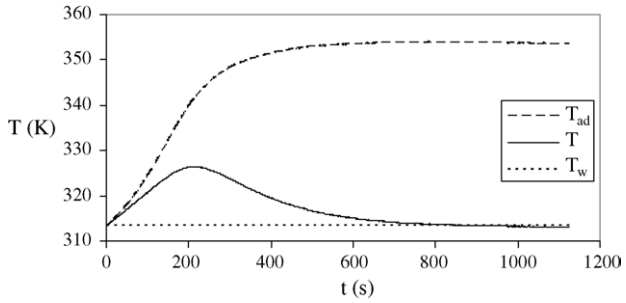

Fig. 9. Temperatures in isoperibolic mode. $[H_2O_2]_0 = 1.8$ M; $[Cr_2O_7]_0 = 0.003$ M; $T_0 = 313$ K.

mixture was continuously agitated with a magnetic stirrer (700 rpm).

5.2. Experimental results

An adiabatic temperature can again be deduced from the thermal variations in the reactor using relation 17. Yet, the adiabatic temperature is this time very different from the temperature in the reactor, because of the best transfer, as can be seen in Fig. 9. Its interest is then to simply calculate the adiabatic temperature rise ΔT_{ad}, to express the variations of conversion according time, and to thus compare varying operating conditions:

$$T_{ad} = T_0 + \Delta T_{ad} X = T_0 + \varphi(T - T_0) + \int_0^t \frac{(T - T_w)}{\tau_c} \tag{31}$$

Effects of the experimental parameters can be compared using the adiabatic temperature. They are the same as those observed in adiabatic mode, and will not be presented here.

5.3. Determination of enthalpy and kinetics expression

The reaction enthalpy has been determined using the adiabatic temperature rise ΔT_{ad}. Its mean value is here:

$$\Delta_r H = -96.1\ \text{kJ mol}^{-1}$$

which is very close the enthalpy determined in the previous section.

The kinetics determination was performed by resolution of the coupled heat and mass balances (relations 25 and 26), of course expressed as a function of the real temperature T in the vessel. This optimization was performed in two times: the kinetics parameters were first determined on the beginnings of curves, using a pseudo zeroth order. Indeed, at the beginning of the experiment, advance is small, the $K[H_2O_2]_0^2(1 - X)^2$ term is large against 1, and thus kinetic law is close to a pseudo zeroth order in peroxide (relation 7), which then no more depends on the equilibrium constant K. At the end of the experiment the two terms are of the same order of magnitude, and thus the reaction depends on the peroxide concentration.

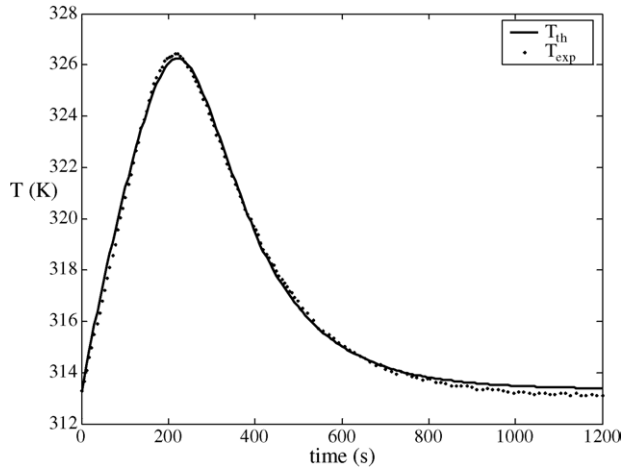

Fig. 10. Experimental and theoretical temperatures during an isoperibolic experiment. $[H_2O_2]_0 = 1.8$ M; $[Cr_2O_7]_0 = 0.003$ M; $T_0 = 313$ K.

Fig. 10 shows the good agreement between theoretical and experimental temperatures for an experiment. The optimized kinetic and equilibrium parameters are finally:

$$k\,(\text{s}^{-1}) = 1.74 \times 10^9 \exp\left(-\frac{6570}{T}\right),$$

$$K\,(\text{L}^2\,\text{mol}^{-2}) = \exp\left(\frac{2725}{T} - 4.91\right) \tag{32}$$

These values are not very different from those obtained in adiabatic mode.

The relative standard deviation is here 1.9×10^{-3} and the mean absolute difference 0.52 K. The uncertainties and determined kinetic and thermodynamic parameters are almost identical to those obtained in batch adiabatic mode. Thus, as batch adiabatic mode as batch isoperibolic mode can both be used to perform kinetic and thermodynamic measurements with the same precision. Another experimental device is presented in the next section.

6. Differential thermal analysis reactors

The reaction was then implemented in two reactors working on the principle of the differential thermal analysis.

The principle of differential thermal analysis (or DTA) consists in the measurement of the heating effects associated with physical and chemical transformations occurring when a substance is heated (or cooled) at a uniform speed. For a batch liquid reaction, two reaction vessels are run in parallel. One is filled with the reaction components and the other one, e.g. with the solvent. The basic signal used for the evaluation is the temperature difference of the two reactor-contents [5].

The interest of working in DTA is to measure, in only one experiment, different phenomena appearing at various temperatures, or multiple kinetic effects, differently activated.

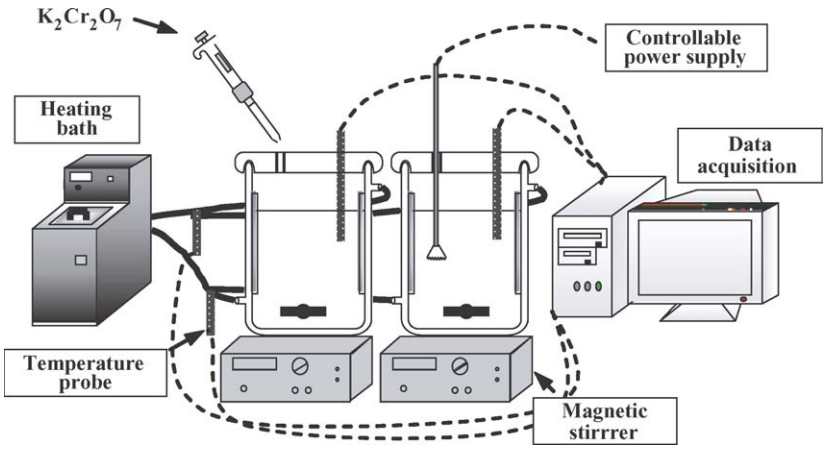

Fig. 11. Experimental setup for the differential thermal analysis mode.

6.1. Protocol

Two identical jacketed vessels, and same as that used in the isoperibolic mode study, were used. The reactional mixture containing hydrogen peroxide without catalyst was placed in the first one, whereas the complete reactional mixture was in the second reactor. The stirring speed was the same in the two reactors (700 rpm) and the initial temperature was sufficiently low so that the reaction did not begin.

A sketch of the experimental setup is presented in Fig. 11. Both vessels are 0.25 L in capacity. The thermal calibration was first realized for both vessels, as for the batch adiabatic and isoperibolic modes. Resolution of the calibration balance (relation 10) shows that both reactors have the same thermal characteristics: $UA = 2.48\ \mathrm{W\,K^{-1}}$ and $\varphi = 1.057$.

6.2. Experimental results

A linear variation of the jacket fluid temperature was then imposed, and the variations of temperatures T_{ref} for the reference vessel and T for the reactor were then recorded. The difference in temperature variations between the two vessels gives a thermal signature of the reaction, and enables the determination of the reaction enthalpy, as well as the kinetic and equilibrium constants for a given reaction pathway.

Defining:

$$T_{\mathrm{d}} = T - T_{\mathrm{ref}} \tag{33}$$

the difference between heat balances in the reactor and the reference vessel (where no reaction occurs) gives:

$$\frac{\Delta T_{\mathrm{ad}}}{\varphi}\frac{\mathrm{d}X}{\mathrm{d}t} = \frac{\mathrm{d}T_{\mathrm{d}}}{\mathrm{d}t} + \frac{T_{\mathrm{d}}(t)}{\tau_{\mathrm{c}}\varphi} \tag{34}$$

which can be integrated, to define an adiabatic temperature:

$$T_{\mathrm{ad}}(t) = T_0 + \Delta T_{\mathrm{ad}}X(t) = T_0 + \varphi T_{\mathrm{d}}(t) + \int_0^t \frac{T_{\mathrm{d}}(t)}{\tau_{\mathrm{c}}}\,\mathrm{d}t \tag{35}$$

The adiabatic temperature is very different from the real temperature, and simply allows, as in isoperibolic mode, to calculate the adiabatic temperature rise or to illustrate the variations of conversion as a function of time. Fig. 12 presents the variations of different temperatures in DTA mode.

6.3. Determination of enthalpy and kinetics expression

The mean reaction enthalpy, determined using the adiabatic temperature rise ΔT_{ad}, is:

$$\Delta_{\mathrm{r}}H = -91.2\ \mathrm{kJ\,mol^{-1}}$$

The kinetics determination was performed by resolution of the coupled heat and mass balances (relations 26, 33 and 34), with given expression of T_{ref} versus time. The optimization was simultaneously realized on five experiments, with same initial concentrations and different jacket temperature variations.

The initial values of the four parameters to be determined were taken from those given in adiabatic mode.

Fig. 13 shows the good agreement between theoretical and experimental temperatures for an experiment. The optimized

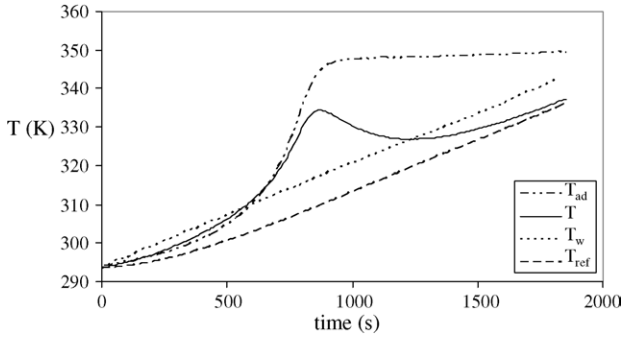

Fig. 12. Temperatures in ATD mode. $[H_2O_2]_0 = 2.7$ M; $[Cr_2O_7]_0 = 0.003$ M; $dT_w/dt = 0.027\ \mathrm{K\,s^{-1}}$.

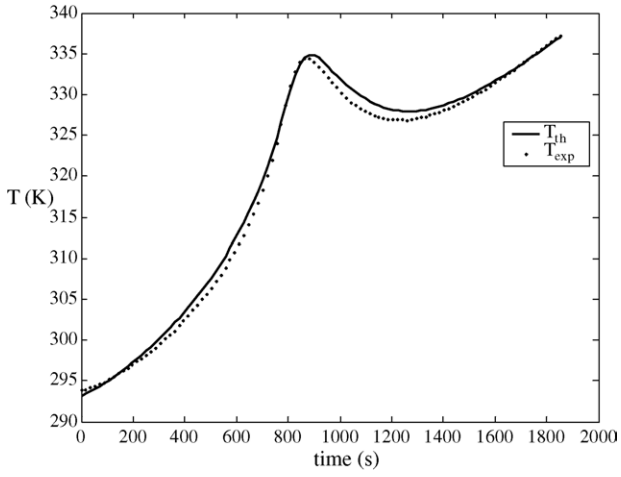

Fig. 13. Experimental and theoretical temperatures in ATD mode. $[H_2O_2]_0 = 2.7$ M; $[Cr_2O_7]_0 = 0.003$ M; $dT_w/dt = 0.027$ K s^{-1}.

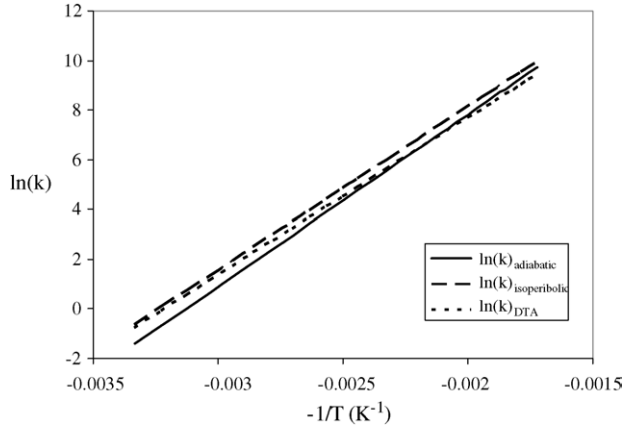

Fig. 14. Comparison of the rate constants for the three operating modes.

kinetic parameters are very close to those obtained in both previous detailed modes:

$$k\,(\mathrm{s}^{-1}) = 6.11 \times 10^8 \exp\left(-\frac{6320}{T}\right),$$

$$K\,(\mathrm{L}^2\,\mathrm{mol}^{-2}) = \exp\left(\frac{2803}{T} - 5.38\right) \quad (36)$$

The relative standard deviation is here 4.1×10^{-3} and the mean absolute difference 1.1 K. Uncertainty is slightly higher as in batch adiabatic or isoperibolic mode, but the agreement between experimental and theoretical values remains very good. The experimental temperature variations are here more important as in previous studied modes, so that some hypotheses (Ellingham approximation, negligible vaporisation heat losses) may be more difficultly validated.

7. Conclusion

The dichromate-catalysed peroxide decomposition has been studied in three operating modes: batch adiabatic reactor, batch isoperibolic reactor, and batch DTA reactors.

The three operating modes make it possible to study the influence of operating conditions, and to measure the reaction kinetics. As a comparison, the three rate constants, determined in the three operating mode, are presented in Fig. 14. The very good agreement between the values shows that any operating mode can be used for the determination of reaction kinetics. The data exploitation is simplest in adiabatic mode, reaction heat dissipation is easier in isoperibolic mode, and the DTA enables to study multiple reactions, occurring at various temperatures. Uncertainties comparison shows that best precision is obtained in batch adiabatic and isoperibolic modes.

It has been shown that the dichromate-catalysed peroxide decomposition kinetics is:

$$r = k\frac{K[H_2O_2]^2[Cr_2O_7{}^{2-}]_0}{1 + K[H_2O_2]^2}$$

where k is described according to the Arrhenius law and K according to the Ellingham approximation.

The thermodynamic and kinetic parameters obtained by the three operating modes are gathered in Table 3. It can be noted that variation between the three operating mode's determined values varies between 4% for the reaction enthalpy and 6 % for the activation energy.

Some average values can finally be proposed:

$$k\,(\mathrm{s}^{-1}) = 1.39 \times 10^9 \exp\left(-\frac{6600}{T}\right),$$

$$K\,(\mathrm{L}^2\,\mathrm{mol}^{-2}) = \exp\left(\frac{2768}{T} - 5.16\right) \quad \text{and}$$

$$\Delta_r H = -94\,\mathrm{kJ\,mol}^{-1}$$

Table 3
Kinetic and thermodynamic parameters

	E/R (K)	Ln (k_0)	$\Delta_r H$ (kJ/mol)	$\Delta H^\circ(T_0)/R$ (K)	$\Delta S^\circ(T_0)/R$ (−)
Adiabatic	6920	21.65	−94.6	−2776	−5.19
Isoperibolic	6570	21.28	−96.1	−2725	−4.91
DTA	6320	20.23	−91.2	−2803	−5.38

The enthalpy value is close to that reported in the literature by Korneeva et al. [6] ($\Delta_r H = -98.4\,\mathrm{kJ\,mol^{-1}}$) and the kinetic rate values are also close to that reported by Brungs et al. [8] in the same operating conditions (indeed, for $T = 313\,\mathrm{K}$, the measured value is here $k = 0.97\,\mathrm{s^{-1}}$, whereas Brungs measured $k = 0.6\,\mathrm{s^{-1}}$).

One of the main facts discovered in the course of this study is that the reaction depends linearly on the initial dichromate concentration. Its order in hydrogen peroxide varies between 0 and 2, depending on operating conditions. The reaction can be managed by playing on two parameters: on one hand the released reaction heat directly depends on the hydrogen peroxide concentration, and on the other hand, the kinetic rate can be increased in increasing the dichromate concentration.

This reaction, of easy implementation, based on non-toxic reactants and products, and whose kinetics and thermicity can be varied, can then be used as a model reaction for the study of thermal stability or thermal runaways of chemical reactors.

References

[1] M.D. Grau, J.M. Nougués, L. Puigjaner, Chem. Eng. J. 88 (2002) 225–232.
[2] R.N. Landau, Thermochim. Acta 289 (1996) 101–126.
[3] O. Ubrich, B. Srinivasan, P. Lerena, D. Bonvin, F. Stoessel, Chem. Eng. Sci. 56 (2001) 5147–5156.
[4] S.M. Rowe, Thermochim. Acta 289 (1996) 167–175.
[5] A. Zogg, F. Stoessel, U. Fischer, K. Hungerbuhler, Thermochim. Acta 419 (2004) 1–17.
[6] N.I. Korneeva, V.I. Shekhobalova, N.I. Kobozev, Russ. J. Phys. Chem. 46 (1972) 210–212.
[7] N.I. Kobozev, V.I. Shekhobalova, N.I. Korneeva, Russ. J. Phys. Chem. 46 (1972) 840–842.
[8] M.P. Brungs, B.G. Madden, P.L. Seage, Chem. Eng. Sci. 43 (1988) 2451–2455.
[9] J.A.C. Frugoni, M. Zepka, A.R. Figueira, A.S. Campos, J. Chem. Educ. 63 (1986) 549.
[10] J. Villermaux, Génie de la Réaction Chimique. Conception et Fonctionnement des Réacteurs, Paris, Tec et Doc, 1995.
[11] J.C. Lagarias, J.A. Reeds, M.H. Wright, P.E. Wright, SIAM J. Opt. 9 (1998) 112–147.